doi:10.1006/jmbi.2001.5436 available online at http://www.idealibrary.com on IDEAL® J. Mol. Biol. (2002) 317, 577–589

JMB

The Role of MeH73 in Actin Polymerization and ATP Hydrolysis

Tomas Nyman[1], Herwig Schüler[1], Elena Korenbaum[1] Clarence E. Schutt[2], Roger Karlsson[1] and Uno Lindberg[1]*

[1]*Department of Cell Biology The Wenner-Gren Institute Stockholm University, S-106 91 Stockholm, Sweden*

[2]*Department of Chemistry Henry H. Hoyt Laboratory Princeton University Princeton, NJ 08544, USA*

**Corresponding author*

In actin from many species H73 is methylated, but the function of this rare post-translational modification is unknown. Although not within bonding distance, it is located close to the γ-phosphate of the actin-bound ATP. In most crystal structures of actin, the δ1-nitrogen of the methylated H73 forms a hydrogen bond with the carbonyl of G158. This hydrogen bond spans the gap separating subdomains 2 and 4, thereby contributing to the forces that close the interdomain cleft around the ATP polyphosphate tail. A second hydrogen bond stabilizing interdomain closure exists between R183 and Y69. In the closed-to-open transition in β-actin, both of these hydrogen bonds are broken as the phosphate tail is exposed to solvent.

Here we describe the isolation and characterization of a mutant β-actin (H73A) expressed in the yeast *Saccharomyces cerevisiae*. The properties of the mutant are compared to those of wild-type β-actin, also expressed in yeast. Yeast does not have the methyl transferase necessary to methylate recombinant β-actin. Thus, the polymerization properties of yeast-expressed wild-type β-actin can be compared with normally methylated β-actin isolated from calf thymus. Since earlier studies of the actin ATPase almost invariably employed rabbit skeletal α-actin, this isoform was included in these comparative studies on the polymerization, ATP hydrolysis, and phosphate release of actin.

It was found that H73A-actin exchanged ATP at an increased rate, and was less stable than yeast-expressed wild-type actin, indicating that the mutation affects the spatial relationship between the two domains of actin which embrace the nucleotide. At physiological concentrations of Mg^{2+}, the kinetics of ATP hydrolysis of the mutant actin were unaffected, but polymer formation was delayed. The comparison of methylated and unmethylated β-actin revealed that in the absence of a methyl group on H73, ATP hydrolysis and phosphate release occurred prior to, and seemingly independently of, filament formation. The comparison of β and α-actin revealed differences in the timing and relative rates of ATP hydrolysis and P_i-release.

Keywords: β-actin mutants; actin isoforms; methylhistidine-73; polymerization; ATP hydrolysis

Introduction

Actin and myosin use free energy provided by hydrolysis of ATP to generate movements in muscle and non-muscle cells. In this process, myosin is believed to be the central force-producing component, whereas actin is seen as a relatively passive element, whose role is to activate the myosin ATPase and bear the load during force generation.[1,2] However, actin also possesses an ATPase

Present addresses: H. Schüler, Department of Biochemistry, NYU Medical Center, 550 First Ave., New York, NY 10016, USA; E. Korenbaum, Institut für Biochemie I, Medizinische Fakultät der Universität Köln, D-50931 Köln, Germany.

Abbreviations used: εATP, 1,N^6-ethenoadenosine 5′-triphosphate; EGTA, ethylene glycol bisaminoethyl ether-*N*,*N*′-tetra acetic acid; F-actin, filamentous actin; G-actin, globular actin; P_i, inorganic phosphate; A_{cc}, critical concentration for polymerization.

E-mail address of the corresponding author: uno@cellbio.su.se

0022-2836/02/040577–13 $35.00/0

activity thought to be important in controlling filament turnover in the cell (reviewed by Chen *et al.*[3]). At low salt concentrations, where the protein exists as monomers in solution, the nucleotide stabilizes the protein. Furthermore, nucleotide hydrolysis and P_i-release during polymerization have been implied to influence the final structure of the filament formed.[4–6] Hydrolysis of ATP on actin and product release might also be intrinsic to force generation during muscle contraction and non-muscle cell motility.[7,8] Therefore, it is of great interest to explore the mechanism by which actin cleaves ATP. We have undertaken a series of investigations examining the role of the amino acid residues in and around the nucleotide-binding site during ATP hydrolysis and P_i-release.[9–11]

Actins from most eukaryotes carry a methylated histidine at position 73.[12–14] This residue is of interest in connection with ATP hydrolysis in actin because its δ1-nitrogen can form a hydrogen bond with the carbonyl group of G158, thereby contacting the G156-V159 loop that chelates the phosphate tail of ATP.[15] This hydrogen-bond bridges the cleft separating the two major domains of actin. The presence of a methyl group on MeH73 confers a positive charge on the side-chain. This enables H73 to participate in a network of electrostatic interactions comprising charged residues E72, MeH73, R177, D179, and R183 that constitute a barrier between the terminal phosphate and the solvent (Figure 1). In the crystal structures, the imidazole of H73 does not make direct contact with the terminal phosphate, but it is in a position to mediate conformational changes in the hairpin loops associated with nucleotide binding thereby governing nucleotide hydrolysis and polymerization.

The methyl group of *S*-adenosyl methionine is transferred to H73 by a methyl transferase that specifically recognizes a peptide *in vivo* corresponding to residues 69-77 of actin.[16] The modification is highly conserved among actins from different species.[17,18] For a long time the only known exception was actin isolated from *Naegleria gruberi* which has an unmethylated histidine 73.[19] However, it was reported recently that the yeasts *Candida albicans* and *Saccharomyces cerevisiae* also lack this modification, suggesting that methyl histidine may be present only in multicellular eukaryotes.[20]

Two highly conserved β-hairpin loops chelate the phosphate tail of ATP between the two major domains of actin. Residues within these loops,

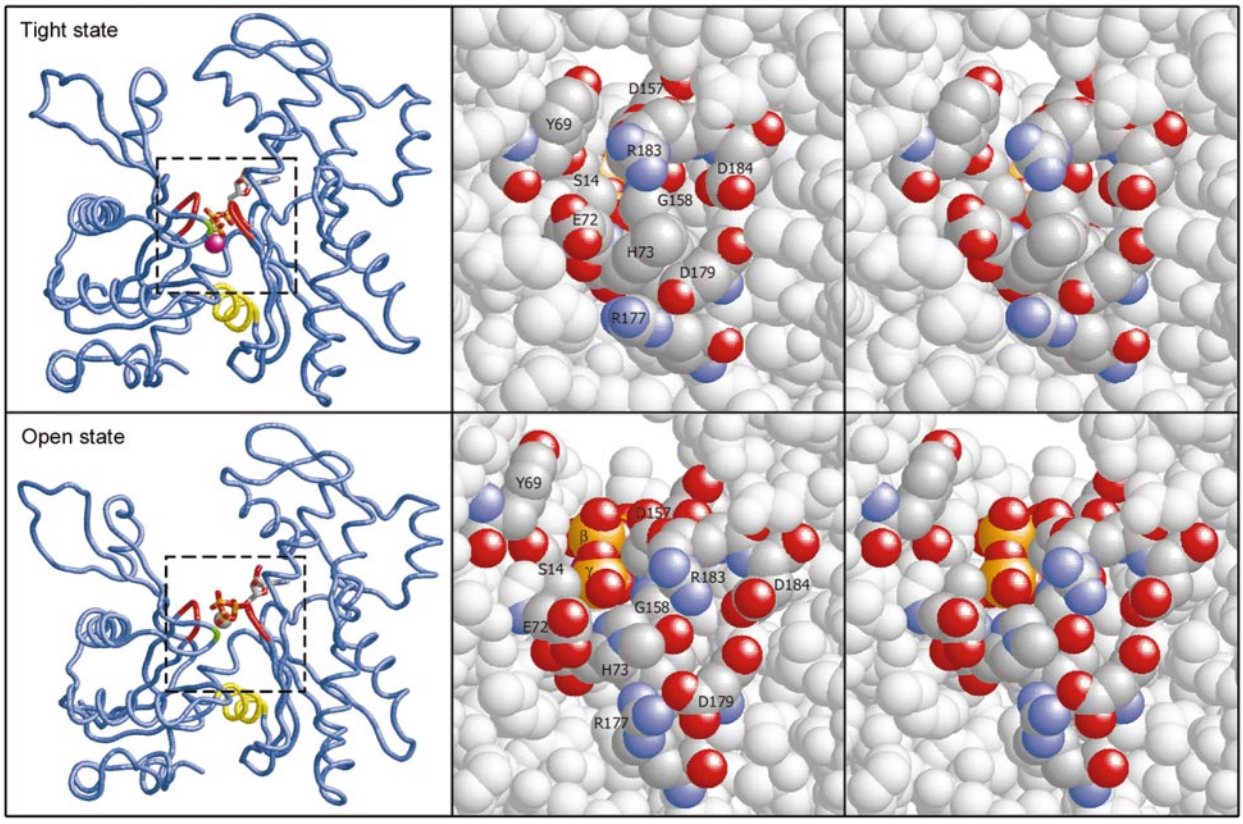

Figure 1. Comparison of the tight and open states of actin in the profilin:β-actin crystals. The overview to the left outlines the area shown in stereo to the right. The barrier residues E72, H73, R177, D179 and R183; the phosphate binding loop-residues S14, D157 and G158; and the hydrogen-bond forming residues Y69 and R183 are labeled. In the open state (bottom row) the β and γ-phosphates (yellow) of the ATP are exposed. In the left overviews, the β-hairpin loops chelating the ATP phosphate tail are colored red, the site of H73 is colored green, and the Q137-S145 helix is colored yellow. All molecular graphics were prepared with RasMol.[66]

S14,[9] D157,[9,21] and V159,[22] and residues in the vicinity of the nucleotide binding site, e.g. R177[9,23] and H73,[24] have been found to be crucial for maintaining the interdomain geometry in actin. However, residues directly involved in the ATP hydrolysis reaction have not yet been identified.

Earlier work on the H73 of actin involves copolymerization of actin mutated at position 73 with wild-type actin,[25,26] and an extensive study of actin where H73 was replaced by several different amino acid residues.[24] However, there have been no reports on the effects of mutating MeH73 on ATP hydrolysis and phosphate release; nor has the significance of methylation for ATPases in general been explored.

Here, chicken β-actin with histidine 73 replaced by either alanine (H73A) or aspartic acid (H73D) was expressed in *S. cerevisiae*. Both mutant actins were purified by DNase I-affinity chromatography, but only the H73A-actin could be isolated from endogenous yeast actin. The characterization of mutated actin (H73A) with respect to DNase I-binding, nucleotide exchange, thermostability, ATPase activity, polymerizability and phalloidin-binding in comparison with non-methylated wild-type actin expressed in *S. cerevisiae* is described here. In addition, non-methylated yeast-expressed wild-type β-actin is compared with methylated mammalian β and α-actin. The results confirm that H73 is important in stabilizing actin in monomeric as well as polymeric form, and that in the absence of a methyl group on the ε2 nitrogen of H73, ATP hydrolysis and phosphate release occurs in advance of polymerization.

The present work also demonstrates that there is a significant difference between the α and β-actin isoforms in the timing of ATP hydrolysis and phosphate release during polymerization. The mechanism of P_i-release and the role of MeH73 in the interdomain relationship in actin are discussed.

Results

Isolation of mutant actins

Chicken β-actin expressed in *S. cerevisiae* was purified from cell extracts using DNase I-affinity chromatography, and separated from endogenous yeast actin by chromatography on hydroxylapatite.[27,28] The H73A mutant actin was eluted from hydroxylapatite at the same ionic strength as wild-type β-actin, well separated from the yeast actin. It was recently shown that yeast actin is not methylated.[20] Also, unlike mammalian actin, yeast-expressed actin retains its N-terminal methionine.[29] To distinguish actins expressed in yeast from wild-type mammalian actin, the following nomenclature will be used: wild-type mammalian β-actin purified from calf thymus is referred to as β-actin$_{cow}$; yeast-expressed wild-type β-actin as β-actin$_{yeast}$ and the H73A mutant actin as H73A-actin. It should be noted that the mammalian β-actin is identical in sequence to chicken β-actin. One actin mutant, H73D actin, bound to DNase I, but conditions for its separation from yeast actin have yet to be found, and it will not be discussed further.

Table 1. Dissociation rate constants for the binding of DNase I and ATP to actin

Property/cation	β-Actin$_{yeast}$	H73A
K_d (DNase I)/Ca^{2+} (nM)	0.28 ± 0.04	6.84 ± 0.38
K_d (DNase I)/Mg^{2+} (nM)	0.66 ± 0.09	5.24 ± 0.47
(k_{-ATP})/Ca^{2+}(s^{-1})	$1.4 \pm 0.2 \times 10^{-3}$	$1.2 \pm 0.4 \times 10^{-2}$
(k_{-ATP})/Mg^{2+} (s^{-1})	$1.6 \pm 0.3 \times 10^{-2}$	$1.5 \pm 0.3 \times 10^{-1}$

The K_d for DNase I:actin interaction was determined using the DNase I inhibition assay. The dissociation rate constant for ATP (k_{-ATP}) was determined from the rate of εATP-incorporation.

Actin:DNase I-interaction

The binding site on actin for DNase I involves parts of both subdomains 2 and 4.[15] Thus, DNase I spans the cleft between the two domains of actin at the (−)-end (so called pointed, or slow growing, end) of the molecule. Earlier work showed that the DNase I-inhibiting activity of actin can be used to probe interdomain relationships in the molecule.[30] It is shown here that the affinity of β-actin$_{yeast}$ for DNase I is closely similar to that of mammalian β and γ-actins, whereas the affinity of H73A-actin for DNase I was greatly decreased (Table 1). Thus, exchanging Ala for His at position 73 causes a significant alteration at the DNase I-binding site, even though H73 is 10 Å away.

Thermostability

Since the alteration in the DNase I-inhibiting activity caused by the H73A-mutation suggests

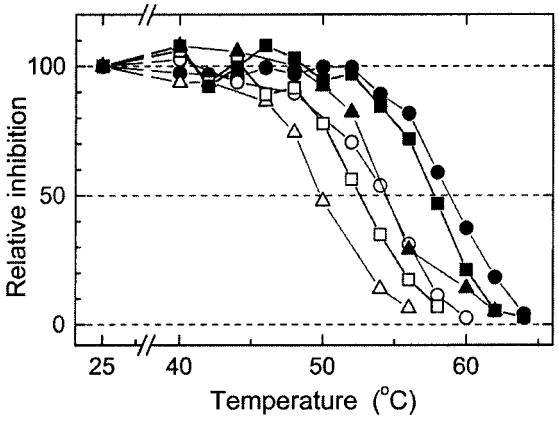

Figure 2. Thermal stability of G-actin. The stability of β-actin$_{yeast}$, β-actin$_{cow}$, and H73A-actin was determined using the DNase I-inhibition assay. The DNase I-inhibition activity at 25 °C was normalized to 100 for each actin. Circles, β-actin$_{yeast}$; squares, β-actin$_{cow}$; triangles, H73A-actin. Filled symbols, Ca-actin; open symbols, Mg-actin.

relative changes in the orientation of the two major domains of actin, it was of interest to investigate the thermal stability of the different actins. For this, the DNase I-inhibition assay was employed as described earlier.[30] As shown in Figure 2, the Mg and Ca-forms of β-actin$_{yeast}$ lost their DNase I-inhibiting activity in a single transition with a $t_{1/2}$ of 55 °C and 58 °C, respectively. The H73A-actin was less stable, with $t_{1/2}$-values of 50 °C and 55 °C for the Ca and Mg-form, respectively. Comparison of the thermal stability of β-actin$_{yeast}$ and β-actin$_{cow}$ showed that the non-methylated, incompletely N-terminally processed β-actin$_{yeast}$ was somewhat more stable than the methylated, N-terminally processed counterpart in both the Mg and Ca-states.

Nucleotide exchange

To investigate whether the H73A-mutation influenced the binding of ATP to actin, measurements of nucleotide exchange rate were performed. For this, ATP-actin was incubated with εATP in the absence of excess ATP, and the increase in fluorescence resulting from εATP binding to actin was monitored. Under the conditions used, including a large excess of εATP, rebinding of ATP is negligible and the rate of incorporation of the fluorescent nucleotide therefore represents the off-rate for ATP (k_{-ATP}).[31] Table 1 shows that for both the Mg and the Ca-form, the k_{-ATP} for H73A-actin was tenfold higher than for β-actin$_{yeast}$.

G-actin ATPase

To evaluate the effect of mutating His73 on the intrinsic ATPase activity of actin, the activities of both the Ca and Mg-forms of β-actin$_{yeast}$ and H73A-actin were examined. Figure 3 shows that β-actin$_{yeast}$ in the Ca-form under non-polymerizing conditions hydrolyzed ATP at a rate of 0.05/hour,

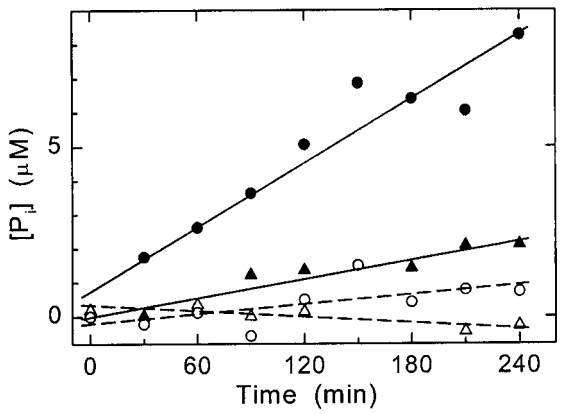

Figure 3. ATPase activity of G-actin. The amount of inorganic phosphate generated by 12 μM Ca- and Mg-actin in buffer G was monitored using the phosphomolybdate precipitation assay. Filled symbols, β-actin$_{yeast}$; open symbols, H73A-actin; circles Mg-actin, triangles, Ca-actin.

whereas the H73A Ca-actin apparently was unable to hydrolyze ATP. In the Mg-form, β-actin$_{yeast}$ exhibited a fourfold higher ATPase activity (0.2/hour) than in the Ca-form, while the H73A-actin in the Mg-form expressed only a weak activity (0.02/hour). Thus, under non-polymerizing conditions, it seems that a histidine residue at position 73 is necessary for actin to hydrolyze ATP.

Polymerization, ATP hydrolysis and P$_i$-release

In 0.1 mM $CaCl_2$ and 100 mM KCl, the β-actin$_{yeast}$ polymerized to steady state in about two hours (Figure 4(a)). The ATP hydrolysis and phosphate release preceded polymerization during the elongation phase. The rate of hydrolysis continued undiminished after steady state of polymerization had been reached. The overall rate of hydrolysis during polymerization was 0.5 h^{-1}. The H73A mutant did not form filaments nor did it hydrolyze ATP under these conditions (Figure 4(d)).

With Mg^{2+} at the high-affinity cation binding site (50 μM $MgCl_2$), and with 100 mM KCl added to the solution (Figure 4(b) and (e)), the β-actin$_{yeast}$ polymerized to steady state in 15 minutes and ATP hydrolysis occurred simultaneously with, or slightly ahead of filament formation as probed by the pyrenyl-assay. The H73A-actin was able to form filaments under these conditions although polymerization did not reach steady state until after 25 minutes. As in the case of β-actin$_{yeast}$ ATP hydrolysis preceded filament formation.

With Mg^{2+} at the high-affinity binding site, and with 1 mM $MgCl_2$ and 100 mM KCl in the solution (Figure 4(c) and (f)), polymerization was faster for both β-actin$_{yeast}$ and the H73A mutant, reaching steady state in 12 and 20 minutes, respectively. The effect of the additional Mg^{2+} on ATP hydrolysis was remarkable in that both actins hydrolyzed ATP well ahead of filament formation, and the amount of ATP consumed at steady state was higher than that expected from the amount of actin added. In these experiments as well as in those of Figure 4(b) and (e), ATP hydrolysis proceeded with the same kinetics for both β-actin$_{yeast}$ as well as H73A-actin, independently of the polymerization rate.

It is interesting that the gain in polymerizability of the H73A-actin (Figure 4(d) and (e)) and the increased rate of filament formation of the β-actin$_{yeast}$ (Figure 4(a) and (b)) apparently are not solely effects of adding Mg^{2+}, since the mere removal of Ca^{2+} by EGTA restored polymerizability to the H73A mutant actin (Figure 5).

S. cerevisiae does not methylate histidine 73 in actin.[24] The availability of methylated β-actin isolated from calf thymus offered the possibility of investigating the specific effect of the methyl group on the imidazole on ATP hydrolysis and phosphate release. Figure 6 shows that with Mg-β-actin$_{cow}$ supplemented with 1 mM $MgCl_2$ and 100 mM KCl, ATP hydrolysis and phosphate

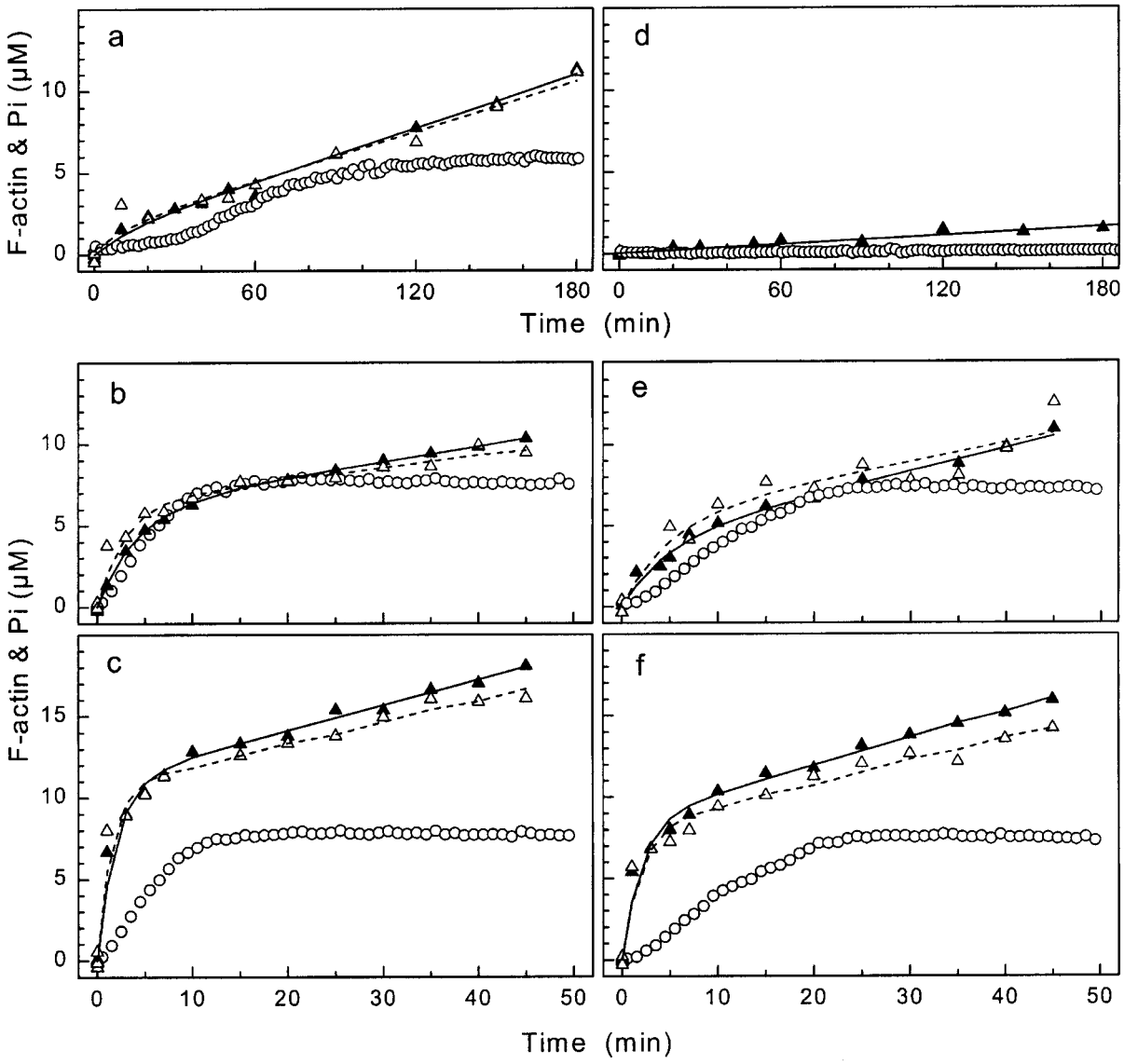

Figure 4. Comparison of β-actin$_{yeast}$ ((a)-(c)) and H73A-actin ((d)-(f)). Filament formation was measured by the pyrenyl-assay and the concomitant formation of inorganic phosphate was determined by TLC. All measurements were performed with 8 μM actin. (a) and (d) Ca-actin + 100 mM KCl. (b) and (e) Mg-actin (50 μM $MgCl_2$) + 100 mM KCl. (c) and (f) Mg-actin + 100 mM KCl and 1 mM $MgCl_2$. Circles, polymerization; filled triangles, ATP hydrolysis; open triangles, P_i-release.

release followed closely the progress of filament formation, whereas β-actin$_{yeast}$ under the same conditions hydrolyzed ATP and released P_i prior to filament formation.

In the polymerization/ATPase experiments described above, P_i-release appeared to occur simultaneously with ATP hydrolysis. Earlier reports with α-actin have described a delay between hydrolysis and P_i-release.[32,33] Thus, it was of interest to use the ATPase and P_i-release assays employed here in a direct comparison between β and α-actins. As seen in Figure 7, α-actin displays a clear delay between hydrolysis and P_i-release, confirming previous observations and demonstrating a clear difference between the muscle and non-muscle actins.

Viscometry

To obtain information about the quality of the polymers formed from the H73A-mutant, filament formation was studied by high shear viscometry (Figure 8). Addition of 1 mM $MgCl_2$ and 100 mM KCl to H73A-actin monomers in the Mg-form led to a viscosity increase after a much longer lag phase than in the case of β-actin$_{yeast}$. Furthermore, both the maximal rate of viscosity increase of the mutant protein and the steady state level of viscosity was significantly lower. Since the A_{cc} of H73A was only slightly increased in comparison with β-actin$_{yeast}$ (Table 2), this suggests that the H73A-mutation affected not only the assembly process, but also the stability of the filaments.

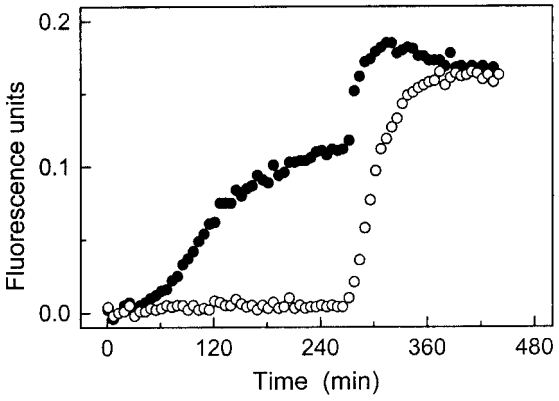

Figure 5. The effect of EGTA on the polymerization of Ca-actin. Filament formation was induced by the addition of 100 mM KCl to 8 μM Ca-actins, and monitored using the pyrenyl assay. After 270 minutes, EGTA was added to 0.2 mM. Filled and open circles denote β-actin$_{yeast}$ and H73A-actin, respectively.

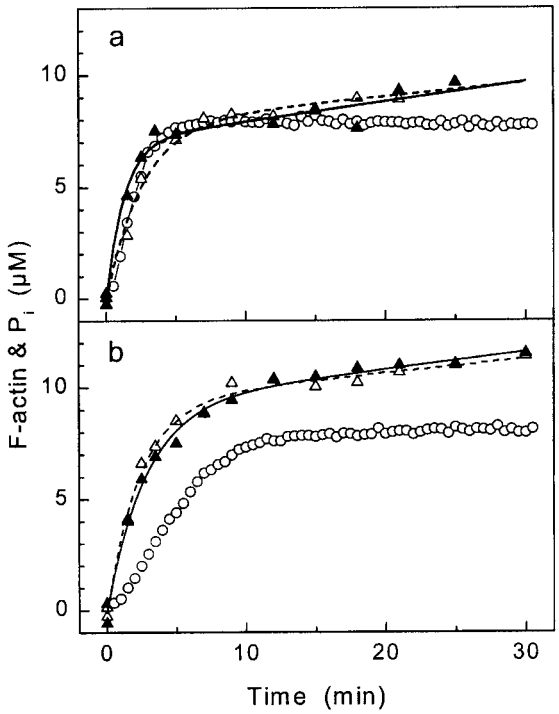

Figure 6. Comparison of β-actin$_{cow}$ and β-actin$_{yeast}$ with respect to polymerization, ATP hydrolysis and phosphate release. Polymerization of Mg-actin (8 μM) was induced by 100 mM KCl and 1 mM $MgCl_2$ and followed using the pyrenyl-assay. Production of inorganic phosphate was monitored by TLC. (a) β-Actin$_{cow}$. (b) β-Actin$_{yeast}$. Circles, polymerization; filled triangles, ATP hydrolysis; open triangles, P_i-release.

Decoration with myosin subfragment 1

The morphology of the filaments formed from H73A-actin could not be distinguished from those of β-actin$_{yeast}$ as analyzed by electron microscopy after negative staining, and the mutant filaments bound myosin-S1 fragments, giving rise to the classical arrowhead structure (not shown).

Binding of phalloidin

Histidine 73 is close to residues G158, R177, and D179, which have been implicated in the binding of phalloidin to actin in the filamentous form.[21] Figure 9 shows the binding of phalloidin to α-actin, β-actin$_{yeast}$ and H73A-actin, as a function of F-actin concentration. The slopes of the binding curves are approximately equal, indicating that the H73A mutation did not severely affect phalloidin binding. The rise of the H73A binding curve occurred at a higher actin concentration, again illustrating the increased A_{cc} of the actin mutant.

Discussion

Conformationally different states of actin

There are biochemical, spectroscopic and electron microscopic observations indicating that the actin monomer has different conformations depending on the status of the actin-bound ATP, the nature of the divalent cation (Ca^{2+} or Mg^{2+}) at the high affinity site or at additional sites, and to the degree of oligomerization.[34,35] Crystallographic investigations on profilin:β-actin have directly demonstrated that actin can exist in a tight and an open state, which differ significantly in conformation.[36,37] The most dramatic difference between the two structures is the opening of the interdomain cleft. It comes about by a 10° rotation of subdomain 1, with the Q137-S145 helix and R335 as pivot points[38,39] (Figure 1), which results in an outward shift of the N12-C17 loop, exposing the phosphate tail of ATP to solution.[37]

Table 2. Critical concentration for polymerization for β-actin$_{yeast}$ and H73A-actin

Cation	Salts added	β-Actin$_{yeast}$ (μM)	H73A (μM)
Ca^{2+}	KCl	2.1	>12
Mg^{2+}	KCl	0.2	0.65
Mg^{2+}	KCl+$MgCl_2$	0.2	0.45

The A_{cc} values were determined by the polymerization of a series of actin concentrations using the pyrenyl-actin assay. The high-affinity cation bound to actin prior to polymerization is given in the first column. In the second column, KCl and $MgCl_2$ refers to 100 and 1 mM, respectively.

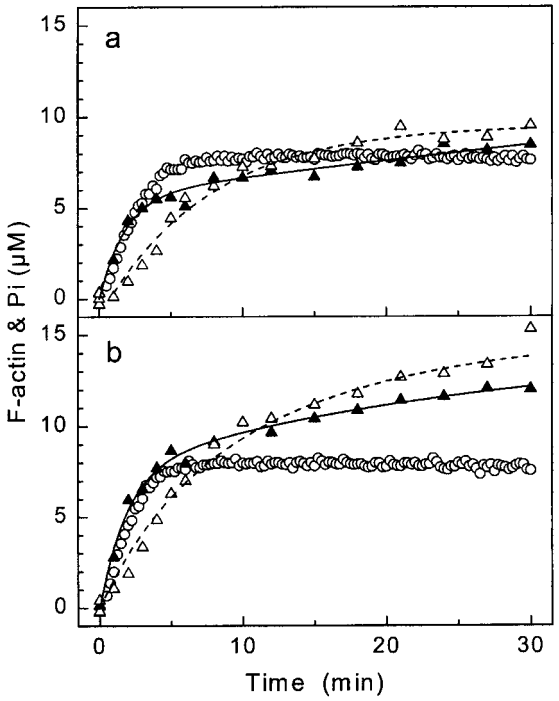

Figure 7. Polymerization and ATPase activity of α-actin. Experiments were performed as in Figures 4 and 6, using 8 μM Mg-actin. (a) Polymerization induced by addition of 100 mM KCl. (b) Polymerization induced by addition of 1 mM $MgCl_2$ and 100 mM KCl. Circles, polymerization; filled triangles, ATP hydrolysis; open triangles, P_i-release. In (a), the graph describing hydrolysis of ATP levels off before an amount of ATP stoichiometric to the amount of actin added has been hydrolyzed, and in both experiments the final amount of P_i released appears to be slightly higher than the total amount of ATP hydrolyzed. These observations were reproducible ($n = 3$), and might be explained by some of the radioactive P_i being trapped in the protein precipitate on the TLC plate. This anomaly, however, does not affect the interpretation of the results.

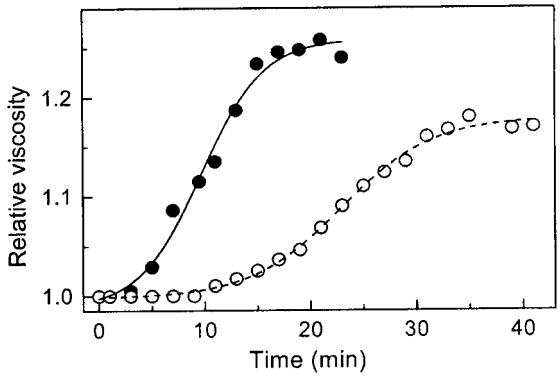

Figure 8. Filament formation analyzed by viscometry. Polymerization of Mg-actin (7 μM) was induced by the addition of salt to 1 mM $MgCl_2$ and 100 mM KCl. Filled and open circles denote β-$actin_{yeast}$ and H73A-actin, respectively.

In the tight state of actin, the terminal phosphates of the nucleotide are bound by the β-hairpin loops, N12-C17 and D156-V159, which protrude into the interdomain cleft from subdomains 1 and 3, respectively. The β-phosphate is hydrogen-bonded to the amide nitrogen atoms of S14, G15, M16, and D157, and the γ-phosphate is bound to amide nitrogen atoms of S14, D157, G158 and V159. In the open state, the hydrogen bond with the amide nitrogen of G15 shifts from the O1 oxygen to the O2 oxygen of the β-phosphate, while the hydrogen bonds of G158 and V159 to the γ-phosphate are broken.[37] In the tight state, there are two hydrogen bonds that span the nucleotide-binding cleft. These two bridging hydrogen bonds, between MeH73 and the carbonyl oxygen of G158 and between the guanido group of R183 and the π-electrons of the ring of Y69,[40] stabilize the closed ATP-form of the actin molecule. In the open state, these hydrogen bonds are broken.

In addition to the loop-phosphate-loop links and the bridging hydrogen bonds, the two major domains of actin are connected through a charge network involving mostly long-chained residues: E72 and MeH73 from one side of the cleft and D157, R177, D179 and R183 from the other. The long-chained residues shield the ATP phosphates from the solvent on one side of the molecule. On the opposite side, there is another set of large residues (M16, K18, K336, and Y337) separating the polyphosphate tail from solvent in both the open and tight states. The transition from the tight to open state does not result in any major changes in this barrier region.

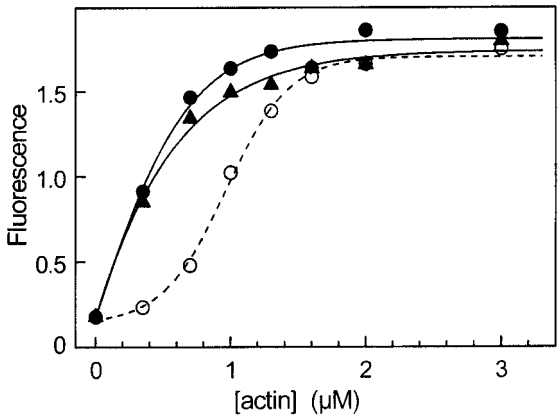

Figure 9. Binding of phalloidin to filamentous actin. Actin at increasing concentrations was polymerized in the presence of 0.35 μM rhodamine phalloidin and 2 mM $MgCl_2$. After the polymerization had reached steady state (two hours) the rhodamine fluorescence was measured. Open circles, H73A-actin; filled circles, β-$actin_{yeast}$; triangles, α-actin.

The structures of different actins determined from crystals of DNase I:α-actin,[15] gelsolin subfragment I:α-actin complexes,[41] gelsolin subfragment I:yeast actin,[42] and gelsolin subfragment I:*Dictyostelium*-actin[42,43] all correspond to the tight state found for β-actin in the profilin:β-actin crystals. It has been noted that the conformation of actin appears relatively unchanged regardless of whether the nucleotide is ATP or ADP, or whether the tightly bound divalent cation is Ca^{2+} or Mg^{2+}. This may seem contradictory in the light of many observations indicating that the actin can attain different conformations depending on the nature of bound ligands.[35,44] The invariability in the α-actin crystal structures may be explained by clamping of the two domains by DNase I-binding across the cleft between subdomains 2 and 4 of actin in the DNase I:actin crystals, or by packing interactions in the case of the gelsolin subfragment 1:α-actin crystals. In the profilin:β-actin crystals, the actin is similarly bridged across subdomain 1 and 2 by a neighboring actin molecule that mimics the contact that is made by DNase I to actin. However, in this case the cleft can open and close in response to changes in ionic conditions made possible through intramolecular hinging and shearing movements that are coordinated between the bound actin molecules.[37,45] It is also known that exchange of ADP and AMP for ATP in the profilin:actin crystals significantly influences their diffraction.[45]

Interdomain relationships in actin

Exchanging ATP with ADP in actin results in a significant reduction in the stability of the protein, and removal of the nucleotide leads to a rather rapid loss in polymerizability.[46] As shown previously, the effects of mutations in the nucleotide-binding cleft on the spatial relationship between the major domains of actin can be evaluated by determining the DNase I-inhibiting activity, thermal stability and nucleotide exchange rate of the mutated protein.[30] The H73A mutation, as well as mutations in the loops binding the phosphate cause significant decreases in the DNase I-inhibiting activity of the actin, whereas the previously described R177D mutation did not. All four mutations (H73A, R177D,[10] S14C,[9] and the double mutation S14C/D157A[9]) made the actin less stable at increased temperature, increased the nucleotide exchange rate, and reduced the rate of polymerisation. This further emphasizes the importance of the non-covalent bonds between the two major domains to the stability and polymerizability of actin. The ATPase activity of the actins, however, was not altered much by the mutations, when assayed in the presence of Mg^{2+}.

The results obtained here with β-actin mutated at histidine 73 are in close agreement with those reported by Yao and co-workers.[24] These investigators reported that replacing H73 with positively charged residues, arginine or lysine, stabilized actin, whereas the introduction of glutamic acid was destabilizing. This is explainable in terms of the coordinating position of H73 in the charge network, illustrated in Figure 1.

Recently, a crystal structure of uncomplexed actin in the ADP state was reported.[47] Actin was kept in a monomeric state by a covalent binding of tetramethylrhodamine maleimide (TMR) to the C terminus. The position of subdomain 2 is different in this structure as compared to previously determined α-actin structures. It has moved *via* a rotation around the same hinge region that is involved in the movement of subdomain 2 in the tight-to-open state transition of profilin:β-actin.[37] However, the rotation of subdomain 1 with respect to subdomains 3 and 4, intrinsic to the opening of the nucleotide binding cleft, is not seen in TMR-actin. The changes of subdomain 2 in TMR-ADP-actin might be due not just to the transition from ATP to ADP state but also to crystal contacts, or to the tight binding of TMR to the base of subdomain 1. Evidence for allosteric coupling between the C terminus and subdomain 2 has been reported earlier.[48,49]

ATPase activity and polymerization

It is commonly held that ATP hydrolysis is linked to the polymerization of actin and that P_i-release takes place only after filaments have formed. The results shown in Figure 7 confirm that this is true for skeletal muscle α-actin. However, the non-muscle β-$actin_{cow}$ is different in this respect, hydrolyzing ATP slightly ahead of the appearance of actin polymers with P_i-release closely following filament formation. This implies that the use of α-actin might not be appropriate in studies of the interactions of non-muscle actin-binding proteins with actin.

In both β-$actin_{yeast}$ and the H73A mutant actin, nucleotide hydrolysis and P_i-release in 1 mM Mg^{2+} occurred well ahead of filament formation and followed closely similar time courses. A comparison of the results shown in Figures 4 and 6 indicates that the main disturbance in the behavior of the β-$actin_{yeast}$ and H73A mutant actin is not so much in the timing of nucleotide hydrolysis itself, as in the delayed appearance of actin polymers. It is well known that adenosine trisphosphate is important in holding actin in a polymerization-competent form, which is illustrated by the three to fivefold slower polymerization of ADP-actin.[50] It is possible that after hydrolysis of ATP, the methylated H73 stabilizes ADP-P_i actin in an ATP-conformation long enough for rapid filament nucleation and elongation to occur. In the cases of β-$actin_{yeast}$ and H73A mutant actin, where H73 is not methylated, hydrolysis of ATP and P_i-release might rapidly convert actin from an ATP-state to the ADP-state. Thus, what is observed in these cases would be the polymerization of ADP-actins, explaining the decreased polymerization rates. This does not exclude the possibility of a coupling between P_i-

release and filament formation in the case of wild-type actins with a methylated H73.

Nucleotide hydrolysis was slowed down in both β-actin$_{yeast}$ and H73A mutant actin under certain conditions, but was largely restored by the addition of Mg^{2+}, whereas polymer formation was much retarded. While it is true that the N terminus of actin is not identical between bovine and yeast-expressed β-actin (the N-terminal methionine of actin is retained in yeast[29]), the reason for the pronounced difference in ATP hydrolysis *versus* polymer formation is more likely due to the lack of the methyl group on H73, or in the case of the H73A mutant to the lack of the whole histidine side-chain.

In the absence of Mg^{2+} (Figure 4(d)), the H73A-actin did not form filaments and ATP hydrolysis was very slow. Adding EGTA under these conditions (Figure 5) restored the polymerizability of the mutant actin even without the addition of Mg^{2+}. Since Ca^{2+} should still be bound at the high affinity site under these conditions, the stimulatory effect of EGTA on the polymerization appears to be due to the withdrawal of Ca^{2+} bound to secondary divalent cation-binding sites, but this effect cannot yet be explained in structural terms. A direct effect of EGTA on the protein cannot be excluded.

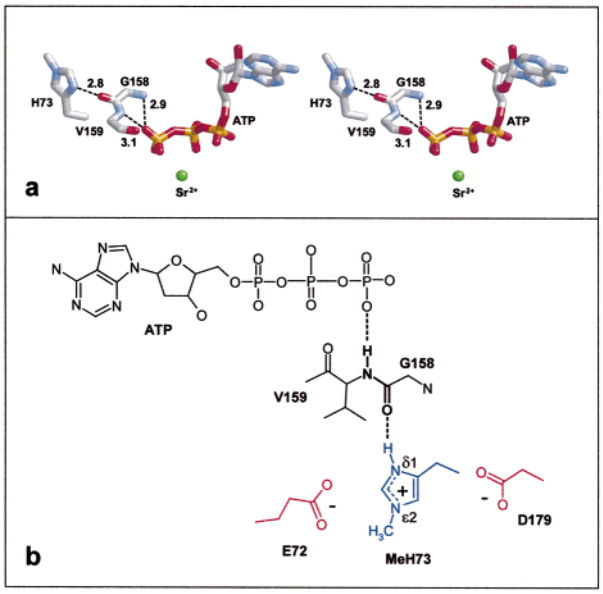

Figure 10. The localization of His73 is similar in all structures of ATP-actin in the tight state. (a) Stereo view showing the hydrogen bonds connecting MeH73, G158, V159, and the γ-phosphate of ATP as shown in the closed state of the profilin:β-actin structure. These hydrogen bonds are all broken in the open state. The numbers denote bond lengths in Å. (b) Schematic drawing showing the electrostatic and hydrogen-bonding interactions of the methylated His73.

The differences between the α-actin and β-actin isoforms seen here might be a reflection of the necessity for a more rapid turnover of actin filaments in motile processes in non-muscle cells, compared with the more static organization of actin filaments in sarcomeres that produce large forces. It is also possible that actin isoform differences in the timing of phosphate release reflect subtle variation in free energy coupling mechanisms underlying force generation in the cytoplasm compared with muscle fibers.

The importance of methylation

The significance of methylation of H73 in actin may be understood from its positioning (Figure 10) and biochemical properties. When the MeHis73 side-chain is protonated, it is fully substituted and carries one positive charge, shared between the two nitrogen atoms. The charge lends salt-bridge character to the MeH73-G158 hydrogen bond, i.e. making it a strong hydrogen bond. Due to π-electron cooperativity, the G158-V159 peptide bond is polarized through the electron-pull from MeH73, increasing the positive nature of the V159 backbone nitrogen. This polarization is further enhanced by the charge on MeH73. This chain of electrostatic interactions strengthens the V159-γ-phosphate hydrogen bond. The positive charge of the protonated MeH73 is also vital for the interactions with its neighbors E72 and D179. Thus, the charged MeH73 side-chain makes contact with three residues, two of them across the base of the nucleotide-binding cleft.

Histidine 12 in bovine pancreatic ribonuclease A is positioned as H73 in actin, with the δ1-nitrogen involved in a hydrogen bond to a backbone oxygen, and the ε2-nitrogen exposed to bulk solution. In this particular histidine, the pK_a of the δ1-nitrogen has been determined to be higher than 8, whilst that of the ε2-nitrogen is around 6.2.[51] This implies that in an unmethylated form of actin, the probability for the H73 ε2-nitrogen to be protonated is low. As a consequence, the interactions between H73 and its neighbors in the charge network are affected, weakening the strength of both the H73-G158 as well as the V159-γ-phosphate hydrogen bond.

It is clear from this analysis that a positively charged residue at position 73 plays a central role in stabilizing a network of electrostatic interactions that bind the polyphosphate tail of ATP in actin. The methylated His in this position in the tight state of actin is hydrogen-bonded *via* its δ1 nitrogen. Therefore, its pK_a is likely to be elevated to more than 8.[51] In the open state, the H73-G158 hydrogen bond is broken and the δ1-nitrogen is exposed to solvent causing a dramatic drop in the pK_a of the δ1-hydrogen. The effect is that the δ1-hydrogen is easily lost into solution and the MeH73 side-chain loses its positive charge, abolishing the possibilities for electrostatic interactions. In conclusion, MeH73 may act as a switch in the cleft

opening mechanism, where cleft opening leads to deprotonization, causing further weakening of the interactions between the two halves of actin.

On the ''front-door'' mechanism of phosphate release in actin

In the presence of Mg^{2+}, the actin ATPase activity is greatly stimulated. Under these conditions, the region near Y69 (R62 - K68) is protected from proteolysis[52] suggesting that the interdomain cleft is closed. Thus, it is possible that the binding of Mg^{2+} to actin stabilizes the tight state of actin allowing nucleotide hydrolysis to take place. Following ATP hydrolysis, breakage of the interdomain hydrogen-bond bridges might allow the opening of the cleft, facilitating release of the γ-phosphate directly into the solvent. This is clearly seen in the tight-to-open transition, in which actin attains a state where the cleft opens up to expose the phosphates (Figure 1).

The phosphate release mechanism envisioned here is quite different from the ''back-door'' mechanism proposed earlier,[53] which involves a solvent channel underneath H73, rather than through the front-door suggested by crystallographic analysis (Figure 1). It was proposed, on the basis of molecular dynamics simulations on yeast actin, that formation of a salt-bridge between H73 and D184 creates a state facilitating P_i-release. This was thought to be part of a series of transfers, involving also R177, that ushers the phosphate ion through a small solvent channel (the back door) connecting the interior of the protein to the bulk solvent. It should be mentioned that the sequence around the nucleotide-binding site in yeast actin is highly conserved, except that yeast actin lacks the methyl group on H73.

As shown in Figure 1, MeH73 and D184 in the crystallographically determined open state of the β-actin, have actually moved further apart, allowing D184 to form a salt-bridge with R183 rather than with H73. Also, in the tight-to-open state transition, R177 of β-actin moves from hydrogen bonding with the backbone atoms of MeH73 to a salt-bridge interaction with the D179. These considerations suggest that changes in actin conformation contributing to an opening of the cleft allow the inorganic phosphate to escape directly into the solution *via* the front-door. Actin-binding proteins could trigger these events.

Materials and Methods

Protein preparation

Site-directed mutagenesis of the chicken β-actin gene, its subcloning into the *S. cerevisiae* expression vector, fermentation of the yeast and isolation of wild-type and mutant β-actins were performed as described.[9,28] It should be noted that chicken β-actin is identical in sequence to mammalian β-actin. Bovine β-actin was isolated from calf thymus profilin:actin,[54] and rabbit skeletal muscle α-actin was isolated as described earlier.[55] The intactness of the actin C termini was verified by the increase in absorbance upon binding of Cu^{2+} to actin[56] as detailed.[9] This is important, since actin that has lost its C-terminal amino-acid residues behaves abnormally.[52,57] Actin with Mg^{2+} at the high affinity cation-binding site was obtained by incubating Ca-actin in buffer G (0.5 mM ATP, 0.1 mM $CaCl_2$, 0.5 mM DTT, 5 mM Tris, pH 7.6) supplemented with 50 μM $MgCl_2$ and 0.2 mM EGTA for ten minutes at room temperature.[58] Pyrene-labeling was done as described.[59] Actin concentration was determined from the absorbance at 290 nm using an absorbance coefficient of 0.63 ml mg^{-1} cm^{-1}.[60]

DNase I-affinity and monomer stability

The affinity of the actin:DNase I-interaction was determined from double-reciprocal plots of the DNase I-inhibition as a function of actin concentration. The DNase I-inhibition was measured at 25 °C using the DNase I-inhibition assay.[61] To determine the thermostability of the H73A-actin monomer, the DNase I-inhibition assay was used as described.[30] Briefly, Ca and Mg-actin as defined above (7.2 μM) in G-buffer were incubated at 40 °C for ten minutes. The temperature was then raised by two degrees every three minutes. Samples of the incubation mixtures were withdrawn and their DNase I-inhibiting activity measured at the end of each three-minute period. The temperature at which the DNase I-inhibiting activity was reduced to 50 % of the activity measured at 25 °C was defined as $t_{1/2}$.

Nucleotide exchange

G-actin (in either the Mg or Ca-form) was freed from excess nucleotide by gel filtration over a Sephadex-G25 column (PD-10, Pharmacia, Sweden) equilibrated with ATP-free G-buffer (with and without 0.2 mM EGTA and 50 μM $MgCl_2$, respectively). Thereafter the protein concentration was adjusted to 6 μM. After addition of 300 μM εATP (Molecular Probes, Eugene, OR), the fluorescence increase at >408 nm ($\lambda_{ex} = 360$ nm) was monitored using a Sigma ZWS II spectrofluorimeter (Biochem Wissenschaftliche Geräte GmbH, Puchheim, Germany). Under these conditions, rebinding of ATP is negligible, and the rate of incorporation of the fluorescent nucleotide represents the off-rate for ATP (k_{-ATP}), e.g. Kinosian *et al*.[31] Estimates of k_{-ATP} were made by first-order curve fitting of the experimental data using Origin (Microcal Software, Northampton, MA).

Polymerization assays

Polymerization of actin was measured with either Ca^{2+} or Mg^{2+} at the high-affinity binding site (Ca and Mg-actin, respectively) at 25 °C and pH 7.6 using the pyrenyl-assay.[59] Polymerization was initiated by addition of either KCl to 0.1 M final concentration, or KCl and $MgCl_2$ to 0.1 M and 1 mM, respectively. Filament formation was monitored by following the increase in fluorescence due to the presence of 2 % pyrene-labeled bovine β/γ-actin ($\lambda_{ex} = 365$ nm; $\lambda_{em} = 410$ nm). Fluorescence measurements were performed using a microplate reader (Fluoroskan II, Labsystems, Finland). The critical concentrations for polymerization of $\beta\text{-actin}_{yeast}$ and H73A-actin in different salt conditions were determined essentially as described.[32,62] Actin was mixed with 2 % pyrene-labeled actin and diluted to concentrations

ranging between 0.02 and 2.0 μM. After addition of polymerizing salts the reaction mixtures were incubated for 14 hours at 20 °C. The resulting steady-state fluorescence was recorded as above.

ATP hydrolysis and phosphate release

The inorganic phosphate formed by the intrinsic ATPase activity of G-actin was measured by the phosphomolybdate procedure of Sugino and Miyoshi[63] as modified by Spudich.[64] All other ATPase experiments were carried out as follows. Actin at 8 μM was equilibrated with [γ-^{32}P]ATP (0.1 Ci/mmol ATP, final activity), $MgCl_2$ and EGTA prior to the onset of filament formation. Polymerization was induced by the addition of 1.0 mM $MgCl_2$ or 100 mM KCl, or both, aliquots of 0.5 μl were withdrawn at different time points and loaded onto TLC plates cut to 4 cm × 8 cm (PEI cellulose F, plastic sheets, Merck, Darmstadt, Germany). The absorption of actin to the cellulose quenched further ATP hydrolysis. The TLC plates were dried thoroughly, developed in 0.2 M NH_4HCO_3 (pH 8), dried and placed in a storage phosphor screen cassette (BAS cassette 2325, Fuji Photo Film Co., ltd) for 20-30 minutes. The phosphor screen was read using a Fujifilm FCA-3000 (Fuji Photo Film Co., ltd), and the relative amounts of $^{32}P_i$ and [γ-^{32}P]ATP were quantified using the program Image Gauge (Fuji Photo Film Co., ltd). The amount of hydrolyzed ATP was calculated as follows: in each sample, the radioactivity of the generated $^{32}P_i$ relates to the total radioactivity ($^{32}P_i$ + [γ-^{32}P]ATP) as the P_i relates to the total amount of ATP added to the buffer, which was 0.5 mM. Thus, the amount of hydrolyzed ATP, expressed in μM is ($^{32}P_i$/total) × 500-t_o, where t_o is the amount of P_i in the reaction mixture immediately prior to the addition of polymerizing salt.

For measurement of phosphate release from polymerizing actin, the reaction mixture was prepared as described for the TLC assay above. At each time point a 30 μl aliquot was withdrawn and placed in a 200 μl filtration filter unit with a molecular cutoff of 30 kDa (Ultrafree-MC, Millipore Corporation, Bedford, MA, USA). The sample was centrifuged for five seconds, to allow for a few μl to pass through the filter. Subsequently 0.5 μl from the filtrate was placed on a TLC plate as above. All release assays was performed simultaneously with ATPase measurements and using the same reaction mixture.

Viscometry

Viscometry was performed at 25 °C in a capillary viscometer (Cannon-Manning 100) with a buffer flow-time of 56 seconds. Measurements were done using 0.7 ml Mg-actin at 7.1 μM. After determination of the flow time of G-actin, polymerization was induced by addition of salt to 100 mM KCl and 1 mM $MgCl_2$. The viscosity was recorded at two-minute intervals.

Phalloidin-binding

Binding of rhodamine-phalloidin to filamentous actin was monitored spectrofluorimetrically ($\lambda_{ex} = 544$ nm; $\lambda_{em} = 590$ nm) using a microplate reader (Fluoroskan II, Labsystems, Finland). This takes advantage of the 20-fold increase in fluorescence of rhodamine-phalloidin upon binding to F-actin.[65]

Acknowledgments

We are grateful for valuable comments given by the reviewers. We acknowledge financial support from the Swedish National Science Research Council (NFR) to U.L. and R.K., from the Swedish Foundation for International Cooperation in Research and Higher Education (STINT) to U.L., and to C.E.S. from the NIH (GM44038).

References

1. Huxley, A. F. & Simmons, R. M. (1971). Proposed mechanism of force generation in striated muscle. *Nature,* **233**, 533-538.
2. Huxley, H. E. (1971). The structural basis of muscular contraction. *Proc. Roy. Soc. London B, Biol. Sci.* **178**, 131-149.
3. Chen, H., Bernstein, B. W. & Bamburg, J. R. (2000). Regulating actin-filament dynamics *in vivo*. *Trends Biochem. Sci.* **25**, 19-23.
4. Janmey, P. A., Hvidt, S., Oster, G. F., Lamb, J., Stossel, T. P. & Hartwig, J. H. (1990). Effect of ATP on actin filament stiffness. *Nature,* **347**, 95-99.
5. Orlova, A. & Egelman, E. H. (1992). Structural basis for the destabilization of F-actin by phosphate release following ATP hydrolysis. *J. Mol. Biol.* **227**, 1043-1053.
6. Lepault, J., Ranck, J. L., Erk, I. & Carlier, M. F. (1994). Small angle X-ray scattering and electron cryomicroscopy study of actin filaments: role of the bound nucleotide in the structure of F-actin. *J. Struct. Biol.* **112**, 79-91.
7. Schutt, C. E. & Lindberg, U. (1992). Actin as the generator of tension during muscle contraction. *Proc. Natl Acad. Sci. USA,* **89**, 319-323.
8. Schutt, C. E. & Lindberg, U. (1998). Muscle contraction as a Markov process. I: energetics of the process. *Acta Physiol. Scand.* **163**, 307-323.
9. Schüler, H., Korenbaum, E., Schutt, C. E., Lindberg, U. & Karlsson, R. (1999). Mutational analysis of Ser14 and Asp157 in the nucleotide-binding site of beta-actin. *Eur. J. Biochem.* **265**, 210-220.
10. Schüler, H., Nyåkern, M., Schutt, C. E., Lindberg, U. & Karlsson, R. (2000). Mutational analysis of arginine 177 in the nucleotide binding site of beta-actin. *Eur. J. Biochem.* **267**, 4054-4062.
11. Schüler, H., Schutt, C. E., Lindberg, U. & Karlsson, R. (2000). Covalent binding of ATPγS to the nucleotide-binding site in S14C- actin. *FEBS Letters,* **476**, 155-159.
12. Asatoor, A. M. & Armstrong, M. D. (1967). 3-methylhistidine, a component of actin. *Biochem. Biophys. Res. Commun.* **26**, 168-174.
13. Johnson, P., Harris, C. I. & Perry, S. V. (1967). 3-methylhistidine in actin and other muscle proteins. *Biochem. J.* **105**, 361-370.
14. Elzinga, M. & Collins, J. H. (1975). The primary structure of actin from rabbit skeletal muscle. Five cyanogen bromide peptides, including the NH2 and COOH termini. *J. Biol. Chem.* **250**, 5897-5905.
15. Kabsch, W., Mannherz, H. G., Suck, D., Pai, E. F. & Holmes, K. C. (1990). Atomic structure of the actin:DNase I complex. *Nature,* **347**, 37-44.
16. Raghavan, M., Lindberg, U. & Schutt, C. (1992). The use of alternative substrates in the characterization

of actin-methylating and carnosine-methylating enzymes. *Eur. J. Biochem.* **210**, 311-318.
17. Vandekerckhove, J. & Weber, K. (1978). Actin amino-acid sequences. Comparison of actins from calf thymus, bovine brain, and SV40-transformed mouse 3T3 cells with rabbit skeletal muscle actin. *Eur. J. Biochem.* **90**, 451-462.
18. Vandekerckhove, J. & Weber, K. (1979). The complete amino acid sequence of actins from bovine aorta, bovine heart, bovine fast skeletal muscle, and rabbit slow skeletal muscle. A protein-chemical analysis of muscle actin differentiation. *Differentiation,* **14**, 123-133.
19. Sussman, D. J., Sellers, J. R., Flicker, P., Lai, E. Y., Cannon, L. E., Szent-Gyorgyi, A. G. & Fulton, C. (1984). Actin of *Naegleria gruberi*. Absence of N tau-methylhistidine. *J. Biol. Chem.* **259**, 7349-7954.
20. Kalhor, H. R., Niewmierzycka, A., Faull, K. F., Yao, X., Grade, S., Clarke, S. & Rubenstein, P. A. (1999). A highly conserved 3-methylhistidine modification is absent in yeast actin. *Arch. Biochem. Biophys.* **370**, 105-111.
21. Belmont, L. D., Patterson, G. M. & Drubin, D. G. (1999). New actin mutants allow further characterization of the nucleotide binding cleft and drug binding sites. *J. Cell Sci.* **112**, 1325-1336.
22. Belmont, L. D., Orlova, A., Drubin, D. G. & Egelman, E. H. (1999). A change in actin conformation associated with filament instability after Pi release. *Proc. Natl Acad. Sci. USA,* **96**, 29-34.
23. Buzan, J. M. & Frieden, C. (1996). Yeast actin: polymerization kinetic studies of wild-type and a poorly polymerizing mutant. *Proc. Natl Acad. Sci. USA,* **93**, 91-95.
24. Yao, X., Grade, S., Wriggers, W. & Rubenstein, P. A. (1999). His73, often methylated, is an important structural determinant for actin. *J. Biol. Chem.* **274**, 37443-37449.
25. Solomon, L. R. & Rubenstein, P. A. (1987). Studies on the role of actin's N tau-methylhistidine using oligodeoxynucleotide-directed site-specific mutagenesis. *J. Biol. Chem.* **262**, 11382-11388.
26. Xia, D., Peng, B., Sesok, D. A. & Peng, I. (1993). Probing actin incorporation into myofibrils using Asp11 and His73 actin mutants. *Cell Motil. Cytoskel.* **26**, 115-124.
27. Segura, M. & Lindberg, U. (1984). Separation of non-muscle isoactins in the free form or as profilactin complexes. *J. Biol. Chem.* **259**, 3949-3954.
28. Karlsson, R. (1988). Expression of chicken beta-actin in *Saccharomyces cerevisiae*. *Gene,* **68**, 249-257.
29. Cook, R. K., Sheff, D. R. & Rubenstein, P. A. (1991). Unusual metabolism of the yeast actin amino terminus. *J. Biol. Chem.* **266**, 16825-16833.
30. Schüler, H., Lindberg, U., Schutt, C. E. & Karlsson, R. (2000). Thermal unfolding of G-actin monitored with the DNase I-inhibition assay stabilities of actin isoforms. *Eur. J. Biochem.* **267**, 476-486.
31. Kinosian, H. J., Selden, L. A., Estes, J. E. & Gershman, L. C. (1993). Nucleotide binding to actin. Cation dependence of nucleotide dissociation and exchange rates. *J. Biol. Chem.* **268**, 8683-8691.
32. Carlier, M. F. & Pantaloni, D. (1986). Direct evidence for ADP-Pi-F-actin as the major intermediate in ATP-actin polymerization. Rate of dissociation of Pi from actin filaments. *Biochemistry,* **25**, 7789-7792.
33. Melki, R., Fievez, S. & Carlier, M. F. (1996). Continuous monitoring of Pi release following nucleotide hydrolysis in actin or tubulin assembly using 2-amino-6-mercapto-7-methylpurine ribonucleoside and purine-nucleoside phosphorylase as an enzyme-linked assay. *Biochemistry,* **35**, 12038-12045.
34. Moraczewska, J., Wawro, B., Seguro, K. & Strzelecka-Golaszewska, H. (1999). Divalent cation-, nucleotide-, and polymerization-dependent changes in the conformation of subdomain 2 of actin. *Biophys. J.* **77**, 373-385.
35. Schüler, H. (2001). ATPase activity and conformational changes in the regulation of actin. *Biochim. Biophys. Acta,* **1549**, 137-147.
36. Schutt, C. E., Myslik, J. C., Rozycki, M. D., Goonesekere, N. C. & Lindberg, U. (1993). The structure of crystalline profilin: β-actin. *Nature,* **365**, 810-816.
37. Chik, J. K., Lindberg, U. & Schutt, C. E. (1996). The structure of an open state of beta-actin at 2.65 Å resolution. *J. Mol. Biol.* **263**, 607-623.
38. Tirion, M. M. & ben-Avraham, D. (1993). Normal mode analysis of G-actin. *J. Mol. Biol.* **230**, 186-195.
39. Page, R., Lindberg, U. & Schutt, C. E. (1998). Domain motions in actin. *J. Mol. Biol.* **280**, 463-474.
40. Levitt, M. & Perutz, M. F. (1988). Aromatic rings act as hydrogen bond acceptors. *J. Mol. Biol.* **201**, 751-754.
41. McLaughlin, P. J., Gooch, J. T., Mannherz, H. G. & Weeds, A. G. (1993). Structure of gelsolin segment 1-actin complex and the mechanism of filament severing. *Nature,* **364**, 685-692.
42. Vorobiev, S. & Almo, S. (1999). Structure of the yeast actin-human gelsolin segment 1 complex, Protein Data Bankentry 1YAG.
43. Matsuura, Y., Stewart, M., Kawamoto, M., Kamiya, N., Saeki, K., Yasunaga, T. & Wakabayashi, T. (2000). Structural basis for the higher Ca(2+)-activation of the regulated actin-activated myosin ATPase observed with *Dictyostelium/Tetrahymena* actin chimeras. *J. Mol. Biol.* **296**, 579-595.
44. Strzelecka-Golaszewska, H. (2001). Divalent cations, nucleotides, and actin structure. *Results Probl. Cell Differ.* **32**, 23-41.
45. Schutt, C. E., Lindberg, U., Myslik, J. & Strauss, N. (1989). Molecular packing in profilin: actin crystals and its implications. *J. Mol. Biol.* **209**, 735-746.
46. Asakura, S. & Oosawa, F. (1960). Dephosphorylation of adenosine triphosphate in actin solution at low concentrations of magnesium. *Arch. Biochem. Biophys.* **87**, 273-280.
47. Otterbein, L. R., Graceffa, P. & Dominguez, R. (2001). The crystal structure of uncomplexed actin in the ADP state. *Science,* **293**, 708-711.
48. DalleDonne, I., Milzani, A. & Colombo, R. (1999). The tert-butyl hydroperoxide-induced oxidation of actin Cys-374 is coupled with structural changes in distant regions of the protein. *Biochemistry,* **38**, 12471-12480.
49. Kim, E. & Reisler, E. (2000). Intermolecular dynamics and function in actin filaments. *Biophys. Chem.* **86**, 191-201.
50. Cooke, R. (1975). The role of the bound nucleotide in the polymerization of actin. *Biochemistry,* **14**, 3250-3256.
51. Tanokura, M. (1983). ^{1}H-NMR study on the tautomerism of the imidazole ring of histidine residues. II. Microenvironments of histidine-12 and histidine-119 of bovine pancreatic ribonuclease A. *Biochim. Biophys. Acta,*, 586-596.
52. Strzelecka-Golaszewska, H., Moraczewska, J., Khaitlina, S. Y. & Mossakowska, M. (1993). Localis-

ation of the tightly bound divalent-cation-dependent and nucleotide-dependent conformation changes in G-actin using limited proteolysis. *Eur. J. Biochem.* **211**, 731-742.
53. Wriggers, W. & Schulten, K. (1999). Investigating a back door mechanism of actin phosphate release by steered molecular dynamics. *Proteins: Struct. Funct. Genet.* **35**, 262-273.
54. Lindberg, U., Schutt, C. E., Hellsten, E., Tjader, A. C. & Hult, T. (1988). The use of poly(L-proline)-Sepharose in the isolation of profilin and profilactin complexes. *Biochim. Biophys. Acta,* **967**, 391-400.
55. Pardee, J. D. & Spudich, J. A. (1982). Purification of muscle actin. *Methods Enzymol.* **85**, 164-181.
56. Lehrer, S. S., Nagy, B. & Gergely, J. (1972). The binding of Cu^{2+} to actin without loss of polymerizability: the involvement of the rapidly reacting -SH group. *Arch. Biochem. Biophys.* **150**, 164-174.
57. Strzelecka-Golaszewska, H., Mossakowska, M., Wozniak, A., Moraczewska, J. & Nakayama, H. (1995). Long-range conformational effects of proteolytic removal of the last three residues of actin. *Biochem. J.* **307**, 527-534.
58. Gershman, L. C., Newman, J., Selden, L. A. & Estes, J. E. (1984). Bound-cation exchange affects the lag phase in actin polymerization. *Biochemistry,* **23**, 2199-2203.
59. Kouyama, T. & Mihashi, K. (1981). Fluorimetry study of N-(1-pyrenyl)iodoacetamide-labelled F-actin. Local structural change of actin protomer both on polymerization and on binding of heavy meromyosin. *Eur. J. Biochem.* **114**, 33-38.
60. Houk, T. W., Jr & Ue, K. (1974). The measurement of actin concentration in solution: a comparison of methods. *Anal. Biochem.* **62**, 66-74.
61. Blikstad, I., Markey, F., Carlsson, L., Persson, T. & Lindberg, U. (1978). Selective assay of monomeric and filamentous actin in cell extracts, using inhibition of deoxyribonuclease I. *Cell,* **15**, 935-943.
62. Tobacman, L. S. & Korn, E. D. (1983). The kinetics of actin nucleation and polymerization. *J. Biol. Chem.* **258**, 3207-3214.
63. Sugino, Y. & Miyoshi, Y. (1964). The specific precipitation of orthophosphate and some biochemical applications. *J. Biol. Chem.* **239**, 2360-2364.
64. Spudich, J. A. (1974). Biochemical and structural studies of actomyosin-like proteins from non-muscle cells. II. Purification, properties, and membrane association of actin from amoebae of *Dictyostelium discoideum*. *J. Biol. Chem.* **249**, 6013-6020.
65. De La Cruz, E. & Pollard, T. D. (1994). Transient kinetic analysis of rhodamine phalloidin binding to actin filaments. *Biochemistry,* **33**, 14387-14392.
66. Sayle, R. & Milner-White, E. J. (1995). RasMol: biomolecular graphics for all. *Trends Biochem. Sci.* **20**, 374-376.

Edited by R. Huber

(Received 1 November 2001; received in revised form 10 January 2002; accepted 14 January 2002)